Supporting Information

Title: Inhibition of Flaviviruses by Targeting a Conserved Pocket on the Viral Envelope Protein

Short title: Validation of a ligand-binding pocket as an antiviral target

Authors: Melissanne de Wispelaere[1,‡], Wenlong Lian[1,‡], Supanee Potisopon[1,†,‡], Pi-Chun Li[2,‡], Jaebong Jang[2], Scott Ficarro[3], Margaret J. Clark[1], Xuling Zhu[1], Jenifer B. Kaplan[1,†], Jared D. Pitts[1], Thomas E. Wales[4], Jinhua Wang[2], John R. Engen[4], Jarrod A. Marto[3], Nathanael S. Gray[2], Priscilla L. Yang[1*].

Affiliations:

[1] Department of Microbiology and Immunobiology, Harvard Medical School.

[2] Department of Biological Chemistry and Molecular Pharmacology, Harvard Medical School and Department of Cancer Biology, Dana-Farber Cancer Institute.

[3] Department of Cancer Biology, Department of Oncologic Pathology, Blais Proteomics Center, Dana-Farber Cancer Institute and Department of Pathology, Brigham and Women's Hospital

[4] Department of Chemistry and Chemical Biology, Northeastern University.

* Correspondence to: priscilla_yang@hms.harvard.edu

† Current addresses: X.Z., Elpidera/Moderna Therapeutics, 500 Technology Square, Cambridge, MA 02139; J.B.K., Abbvie Bioresearch Center, Worcester, MA; S.P. Bioaster, 40 Avenue Tony Garnier, 69007, Lyon, France.

‡ Contributed equally

Figure S1. IC_{90} value determination, related to Figure 1. Antiviral activity against dengue virus 2 NGC was measured in infectivity assays in which compound treatment was limited to preincubation with the viral inoculum and during the one hour initial infection as described in Figure 1A. Viral yield at twenty-four hours, corresponding to a single round of infection, was taken as a metric of productive viral entry twenty-four hours prior. IC_{90} values were determined by non-linear regression analysis of single-cycle viral yield data. Data listed in the table in Figure 1A are the average and standard deviation of independent experiments performed $n \geq 2$. Plots shown here and in Figure 1A are representative data from one of the $n \geq 2$ independent experiments with error bars indicating the standard deviation for experimental replicates within that experiment.

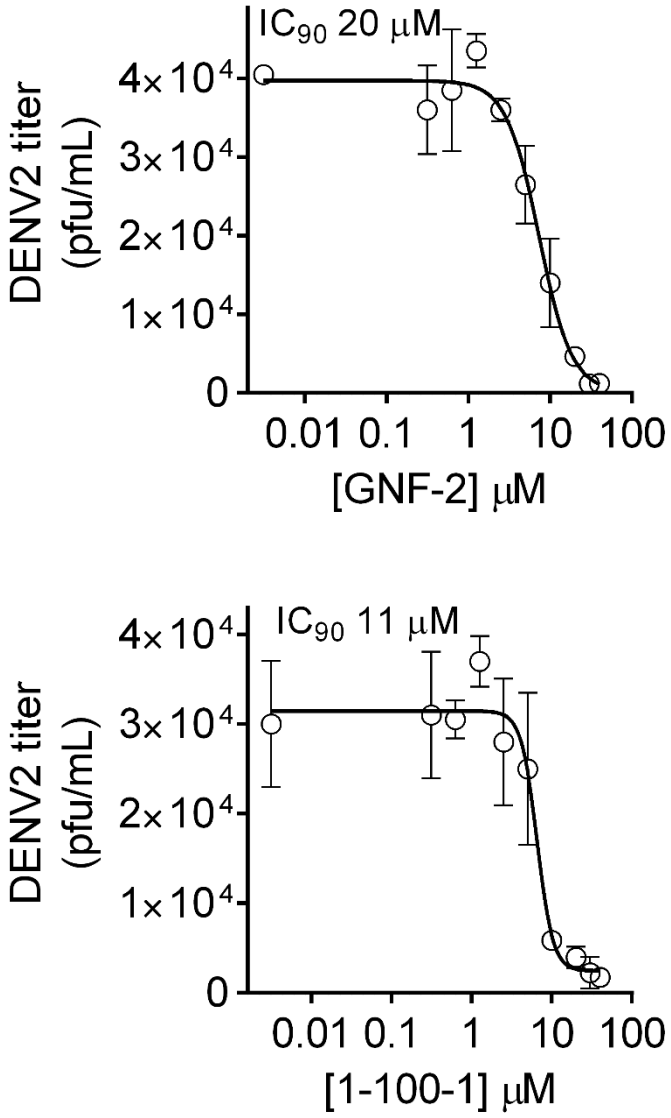

Figure S2. Data for additional compounds in the capsid protection assay to detect fusion of dengue virions with liposomes, related to Figure 1. Fusion of DENV2 virions with synthetic liposomes encapsulating trypsin is triggered by low pH (see schematic in Fig. 1C). Formation of a fusion pore allows trypsin to traffic from the interior of the liposome to the interior of the virion and leads to digestion of the core protein (C) while the envelope protein (E) on the exterior of the virion remains intact. **(A)** Western blot analysis of the reactions for C and E shows that compound 7-148-6 protects core from digestion upon exposure of the virion-liposome mixture to acidic pH, indicating concentration-dependent inhibition of viral fusion. 7-148-6 at concentrations of 10, 20, 30, and 40 μM. **(B)** Additional 2,4-disubstituted pyrimidines (2-12-2, 8-24-3) and 4,6-disubstituted pyrimidines (GNF2, 1-100-1, 1-97-3) also protect core from digestion, indicating inhibition of fusion. GNF2 concentrations were 5, 10, 20, and 40 μM. The other compounds were present at final concentrations of 10 μM. Concentrated supernatant from hybridoma 4G2 expressing an antibody that recognizes the fusion peptide of dengue virus was used as a positive control.

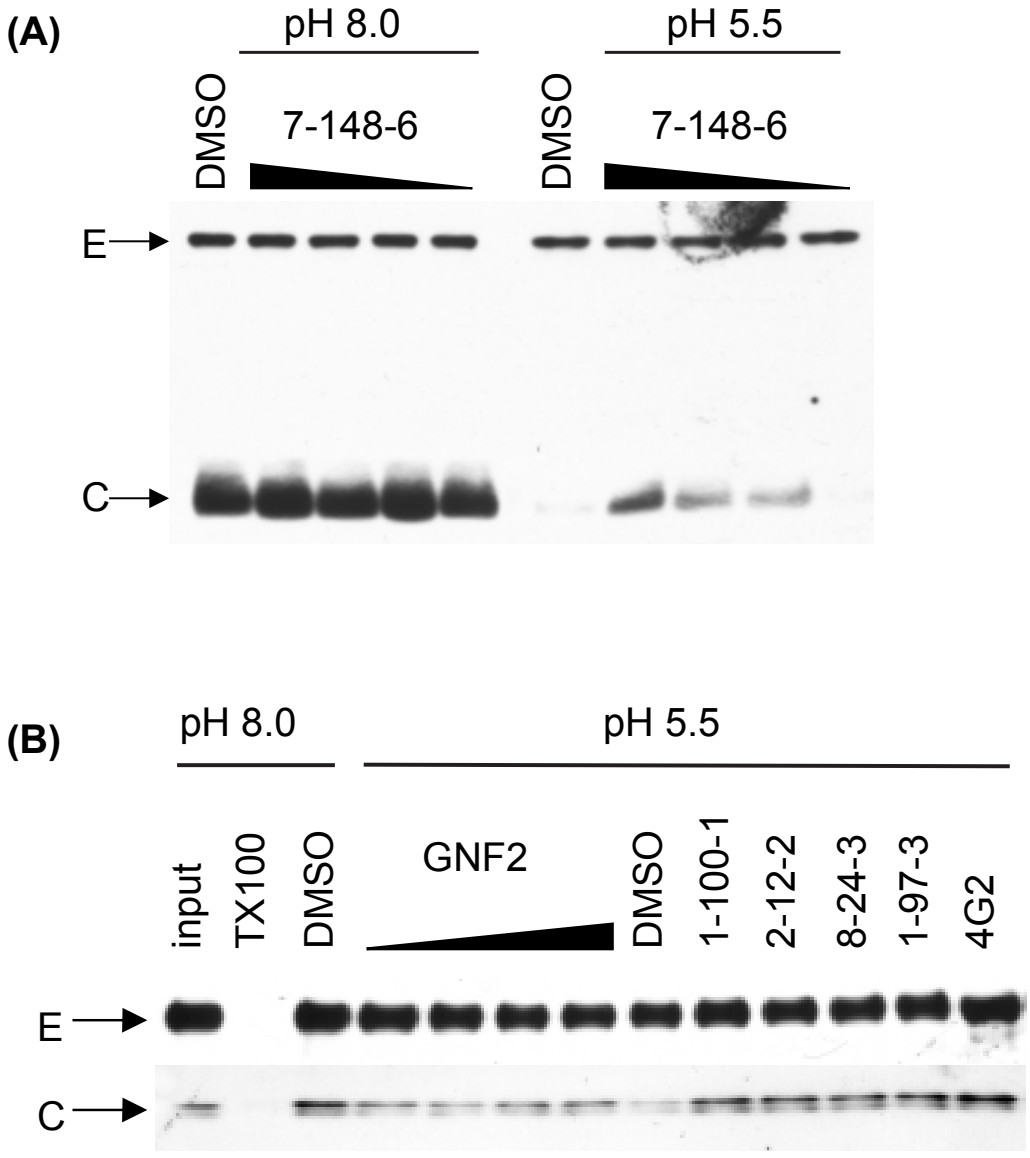

Figure S3. The E-M196V substitution reduces sensitivity of dengue virus entry to inhibition by 2,4-disubstituted pyrimidine 2-12-2 and reduces affinity of E's interaction with 2-12-2, related to Figure 2. **(A)** Antiviral activity was measured in infectivity assays in which compound treatment was limited to preincubation with the viral inoculum and during the one hour initial infection as described in Fig. 1A. Single-cycle viral yield at twenty-four hours post-infection was taken as a metric of successful viral entry twenty-four hours prior. Data are normalized to the DMSO-treated controls and are presented as bar plots as we lacked enough points to perform non-linear regression analysis. Representative data are shown for $n \geq 2$ independent experiments with error bars indicating the standard deviation for experimental replicates within that experiment. **(B)** K_D values for 2-12-2's interaction with DENV2 sE wildtype and sE-M196V were determined by biolayer interferometry. Due to the limitations of compound solubility, we were unable to saturate binding of 2-12-2 with E-M196V and a lower bound has been estimated. Representative data for one experiment are shown with the average and standard deviation for $n \geq 2$ independent experiments presented in the figure legend.

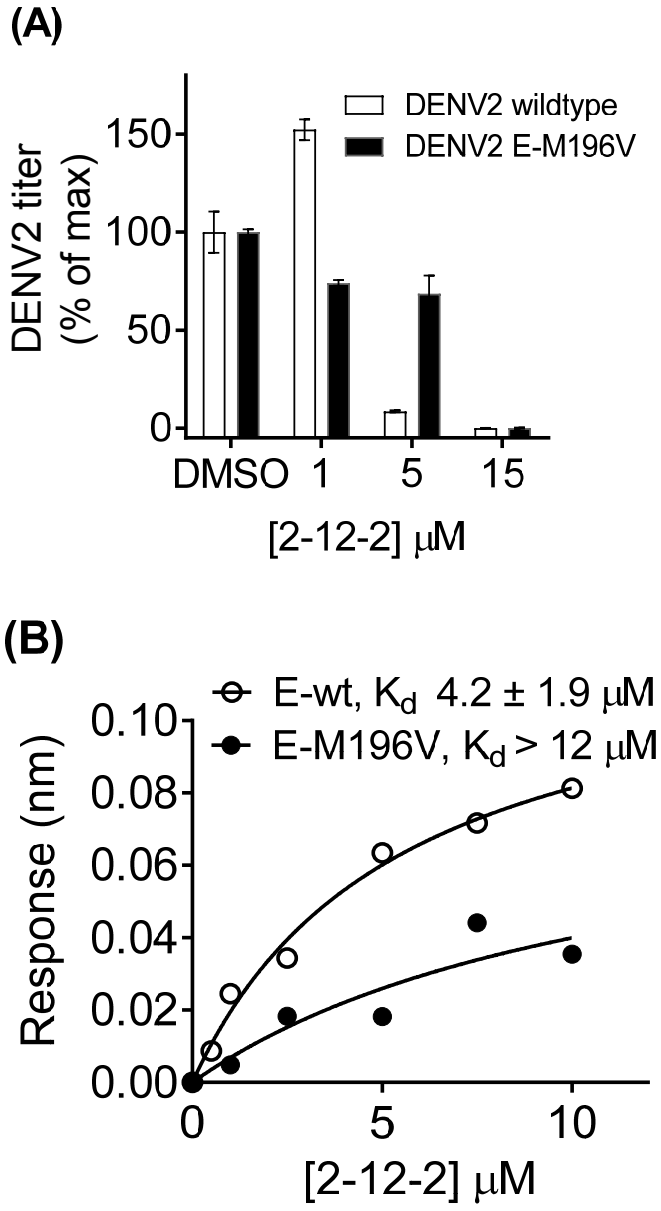

Figure S4. Sensitivity of the DENV2 E-M196V virus to 4,6-disubstituted pyrimidine GNF2, related to Figure 2. IC_{90} values for 4,6-disubstituted pyrimidine **GNF2** against DENV2 NGC and the DENV2 NGC E-M196V viruses were measured as described in Fig. 1A. Single-cycle viral yields were normalized to the titers of the DMSO-treated controls. Due to the limitations of compound solubility, we were unable to saturate binding of **GNF2** with E-M196V and a lower bound has been estimated. Representative data are shown for $n \geq 2$ independent experiments with error bars indicating the standard deviation for experimental replicates in a given experiment. The IC_{90} value presented in the figure legend is the average and standard deviation for $n \geq 2$ independent experiments.

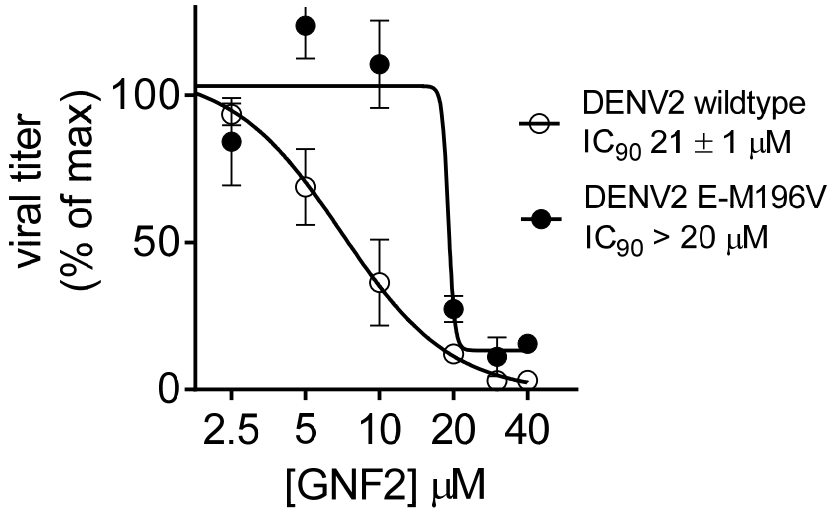

Figure S5. Inhibition of ZIKV and JEV by representative disubstituted pyrimidine inhibitors of DENV2 sE, related to Figure 5. Antiviral activity was measured in infectivity assays in which compound treatment was limited to preincubation with the viral inoculum and during the one hour initial infection as described in Fig. 1A. Viral yield at twenty-four hours, corresponding to a single round of infection, was taken as a metric of productive viral entry twenty-four hours prior. IC_{90} values were determined by non-linear regression analysis of single-cycle viral yield data. Representative data are shown for independent experiments performed $n \geq 2$ times. Error bars indicate the standard deviation for experimental replicates within a given experiment.

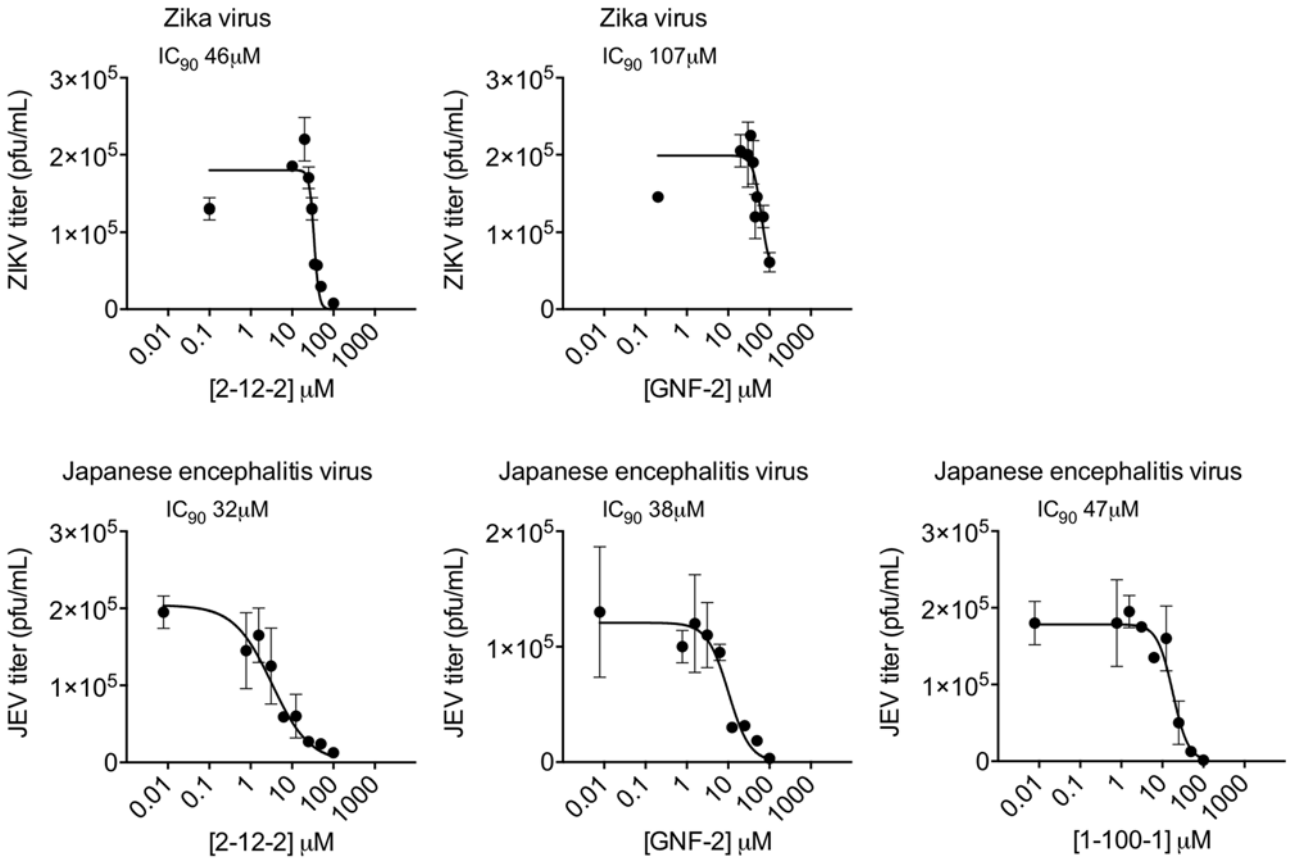

Table S1. Equilibrium dissociation constants (Kd) for interaction of recombinant DENV2 sE proteins with representative inhibitors related to Figure 4. Values are in micromolar (μM) and represent the average of $n \geq 2$ experiments except where noted. For cases in which we were unable to saturate inhibitor-binding but observed clear concentration-dependent inhibitor binding to sE, a lower bound for the Kd is provided based on the fit of available data and the highest concentrations that yielded well-behaved data in the biolayer interferometry experiments. "N.D." indicates that we were unable to measure a Kd value due to absence of reliably quantifiable signal over background in biolayer interferometry experiments, presumably due to low affinity of the compound for the protein and or aggregation of the compound. "*" indicates that we observed concentration-dependent binding but could not fit the data due to poor signal-to-background.

protein	Inhibitor series				
	2,4-diamino pyrimidine		4,6-disubstituted pyrimidine		cyanohydrazone
	7-148-6	**2-12-2**	**GNF2**	**1-100-1**	**3-110-22**
wildtype sE	6.1 ± 1.8 *n* = 4	4.2 ± 1.9 *n* = 6	0.7 ± 0.3 *n* = 4	1.1 *n* = 1	0.6 ± 0.2 *n* = 3
sE-T171A	1.7 ± 0.8 *n* = 2	6.5 ± 2.1 *n* = 2	0.3* *n* = 1	2.9 ± 0.2 *n* = 2	0.2 ± 0.1 *n* = 2
sE-F193L	> 18 *n* = 2	> 32/N.D. *n* = 2	N.D. *n* = 3	0.4 ± 0.1 *n* = 2	1.6 ± 0.6 *n* = 2
sE-M196V	> 13 *n* = 6	> 12 *n* = 4	> 11 *n* = 2	N.D. *n* = 4	> 85 *n* = 2
sE-Q200A	> 70 *n* = 1	>1500/N.D. *n* = 2	N.D. n=1	> 26/N.D. *n* = 2	N.D. *n* = 1
sE-Q200E	1.4 ± 0.3 *n* = 2	2.2 ± 2.6 *n* = 2	1.0 ± 1.1 *n* = 2	1.4 ± 0.1 *n* = 2	1.9 ± 1.7 *n* = 2
sE-Q271A	N.D. *n* = 2	N.D. *n* = 2	N.D. *n* = 2	N.D. *n* = 2	N.D. *n* = 2
sE-Q271E	0.8 ± 0.02 *n* = 2	2.1 ± 2.1 *n* = 2	0.5 ± 0.1 *n* = 2	N.D. *n* = 2	N.D. *n* = 2
sE-M272S	> 20/N.D. *n* = 2	> 19/> 20 *n* = 2	N.D. *n* = 2	N.D. *n* = 2	N.D. *n* = 2
sE-F279S	> 24/N.D. *n* = 2	> 20 *n* = 1	N.D. *n* = 2	N.D. *n* = 1	0.1* *n* = 1

Table S2. List of oligonucleotides used in this study related to site-directed mutagenesis and qPCR assay in the STAR Methods section.

Sequence	Use
5'-GCCTCGACTTCAATGAGGTGGTGTTGTTGCAGATG-3’	Introduce the E-M196V mutation in pCDNA6.2-D2.CprME
5'-CATCTGCAACAACACCACCTCATTGAAGTCGAGGC-3’	Introduce the E-M196V mutation in pCDNA6.2-D2.CprME
5’-AACGCGGCCTCTTCTTATTT-3’	qPCR amplification of *Renilla* luciferase gene
5’-GTCTGGTATAATACACCGCG-3'	qPCR amplification of *Renilla* luciferase gene
5’-AATATGCTGAAACGCGAGAGA-3’	qPCR amplification of DENV2
5’-GGGATTGTTAGGAAACGAAGG-3’	qPCR amplification of DENV2
5’-CAGAAGCCAAAGCACCTGCCACTCTAAGG-3’	Introduce the E-Q52A mutation in pFastBac-DENV2-sE-AviTag
5’-CCTTAGAGTGGCAGGTGCTTTGGCTTCTG-3’	Introduce the E-Q52A mutation in pFastBac-DENV2-sE-AviTag
5’-GAGTTCCATCGCAGAAGCAGAGTTG-3’	Introduce the E-T171A mutation in pFastBac-DENV2-sE-AviTag
5’-CAACTCTGCTTCTGCGATGGAACTC-3’	Introduce the E-T171A mutation in pFastBac-DENV2-sE-AviTag
5’-GAACGGGCCTCGACCTCAATGAGATGGTG-3’	Introduce the E-F193L mutation in pFastBac-DENV2-sE-AviTag
5’-CACCATCTCATTGAGGTCGAGGCCCGTTC-3’	Introduce the E-F193L mutation in pFastBac-DENV2-sE-AviTag
5’-CCTCGACTTCAATGAGGTGGTGTTGCT GC-3’	Introduce the E-M196V mutation in pFastBac-DENV2-sE-AviTag
5’-GCAGCAACACCACCTCATTGAAGTCGAGG-3’	Introduce the E-M196V mutation in pFastBac-DENV2-sE-AviTag
5’-GATGGTGTTGCTGGCAATGGAAAATAAAGCTTGGC-3’	Introduce the E-Q200A mutation in pFastBac-DENV2-sE-AviTag
5’-GCCAAGCTTTATTTTCCATTGCCAGCAACACCATC-3’	Introduce the E-Q200A mutation in pFastBac-DENV2-sE-AviTag
5’-GATGGTGTTGCTGGAAATGGAAAATAAAGCTTGGC-3’	Introduce the E-Q200E mutation in pFastBac-DENV2-sE-AviTag
5’-GCCAAGCTTTATTTTCCATTTCCAGCAACACCATC-3’	Introduce the E-Q200E mutation in pFastBac-DENV2-sE-AviTag
5’-GGGGCCACAGAAATCGCGATGTCATCAGG-3’	Introduce the E-Q271A mutation in pFastBac-DENV2-sE-AviTag
5’-CCTGATGACATCGCGATTTCTGTGGCCCC-3’	Introduce the E-Q271A mutation in pFastBac-DENV2-sE-AviTag
5’-GCCACAGAAATCCAAAGCTCATCAGGAAAC-3’	Introduce the E-M272S mutation in pFastBac-DENV2-sE-AviTag
5’-GTTTCCTGATGAGCTTTGGATTTCTGTGGC-3’	Introduce the E-M272S mutation in pFastBac-DENV2-sE-AviTag
5’-CAGGAAACTTACTGTCCACAGGACATCTCAAGTGC-3’	Introduce the E-F279S mutation in pFastBac-DENV2-sE-AviTag
5’-GCACTTGAGATGTCCTGTGGACAGTAAGTTTCCTG-3’	Introduce the E-F279S mutation in pFastBac-DENV2-sE-AviTag